

Synthesis, Crystal Structures and Third-Order Nonlinear Optical Properties of Two Novel Ferrocenyl Schiff-Base Complexes $[\text{Ag}(\text{L})_2](\text{NO}_3)(\text{MeOH})(\text{EtOH})$ and $[\text{HgI}_2(\text{L})]$ $\{\text{L} = 1,2\text{-Bis}[(\text{ferrocen-1-ylmethylene})\text{amino}]\text{ethane}\}$

Hongwei Hou,^{*,[a]} Gang Li,^[a] Yinglin Song,^[b] Yaoting Fan,^[a] Yu Zhu,^[a] and Lu Zhu^[a]

Keywords: Schiff bases / Silver / Mercury / Nonlinear optics

Two novel ferrocenyl complexes $[\text{Ag}(\text{L})_2](\text{NO}_3)(\text{MeOH})(\text{EtOH})$ (**1**) and $[\text{HgI}_2(\text{L})]$ (**2**) $\{\text{L} = 1,2\text{-bis}[(\text{ferrocen-1-ylmethylene})\text{amino}]\text{ethane}\}$ have been prepared and structurally characterized by means of X-ray single crystal diffraction. The central ion, silver(I) or mercury(II), has a distorted tetrahedral environment, the silver(I) ion coordinates with two L, and the mercury(II) ion binds one L and two iodine atoms. Their third-order nonlinear optical (NLO) properties were determined by Z-scan techniques in DMF solution. The results indicate that the two complexes exhibit very strong

NLO absorption and strong self-focusing effects. The third-order NLO absorptive coefficients a_2 are $1.34 \times 10^{-8} \text{ m W}^{-1}$ for **1** and $3.1 \times 10^{-9} \text{ m W}^{-1}$ for **2**. The refractive indexes n_2 for the two complexes are 1.15×10^{-18} and $8.02 \times 10^{-19} \text{ m}^2 \text{ W}^{-1}$, respectively. The hyperpolarizability γ values are calculated to be $2.68 \times 10^{-30} \text{ esu}$ for **1** and $1.44 \times 10^{-30} \text{ esu}$ for **2**. The γ values are several orders of magnitude larger than those of the reported aryl and vinyl derivatives of ferrocene. (© Wiley-VCH Verlag GmbH & Co. KGaA, 69451 Weinheim, Germany, 2003)

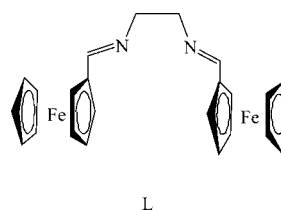
Introduction

Ferrocene-containing compounds are currently receiving much attention due to their increasing role in the rapidly growing area of materials science. They have been used as homogeneous catalysts for various processes,^[1] molecular sensors,^[2] and molecular magnetic^[3] and nonlinear optical materials.^[4] In particular, several studies have been made on the nonlinear optical properties of ferrocene derivatives^[4] since the first report that (*E*)-1-ferrocenyl-2-(*N*-methylpyridinium-4-yl)ethylene iodide and (*Z*)-1-ferrocenyl-2-(4-nitrophenyl)ethylene have large second harmonic generation efficiencies (220 and 62 times that of urea, respectively).^[5]

Ferrocenyl Schiff bases as very important ferrocene derivatives have been studied in this context. Several groups have reported the NLO properties of various monoferrocenyl Schiff bases and bidentate diferrocenyl Schiff bases, but most have focused on second-order NLO properties of those compounds.^[6–10] To the best of our knowledge, there are no reports on the third-order NLO properties of this type of compounds and the corresponding complexes.

Conversely, although the bidentate ferrocenyl Schiff base 1,2-bis[(ferrocen-1-ylmethylene)amino]ethane (L) has pre-

viously been prepared, its metal complexes are quite scarce due to its spontaneous hydrolytic degradation. However, a series of metal complexes with the parent amine of L, 1,2-bis[(ferrocenylmethyl)amino]ethane, have been obtained.^[11–13] The only known complex containing L appears to be the $[\text{ZnCl}_2(\text{L})]$ complex recently described by Li et al.^[14] It is noteworthy that the syntheses of Ag- or Hg-containing ferrocenyl complexes are difficult, due mainly to the instability of Ag^{I} in solution and the poor solubility of Hg^{II} in ordinary solvents. To obtain Ag- or Hg-containing ferrocenyl compounds and find better third-order NLO materials, we utilized the reaction of L with Ag or Hg to synthesize two novel complexes, $[\text{Ag}(\text{L})_2](\text{NO}_3)(\text{MeOH})(\text{EtOH})$ (**1**) and $[\text{HgI}_2(\text{L})]$ (**2**), and further determined their third-order NLO properties using Z-scan techniques. The results reveal that both complexes have very strong third-order NLO absorptive and refractive properties in DMF solution. The hyperpolarizability γ values are calculated to be $2.68 \times 10^{-30} \text{ esu}$ and $1.44 \times 10^{-30} \text{ esu}$ for **1** and **2**, respectively.



^[a] Department of Chemistry, Zhengzhou University, Zhengzhou, 450052, P. R. China
Fax: (internat.) + 86-371/7761744
E-mail: houghongw@zzu.edu.cn

^[b] Department of Physics, Harbin Institute of Technology, Harbin, 150001, P. R. China

Results and Discussion

Crystal Structure of $[\text{Ag}(\text{L})_2](\text{NO}_3)(\text{MeOH})(\text{EtOH})$ (1)

The molecular structure of complex **1** was determined by single-crystal X-ray diffraction analysis. The asymmetric unit contains an $[\text{Ag}(\text{L})_2]^+$ cation, one NO_3^- anion, and one crystallization molecule each of methanol and ethanol. The perspective view of the cation of **1** is illustrated in Figure 1.

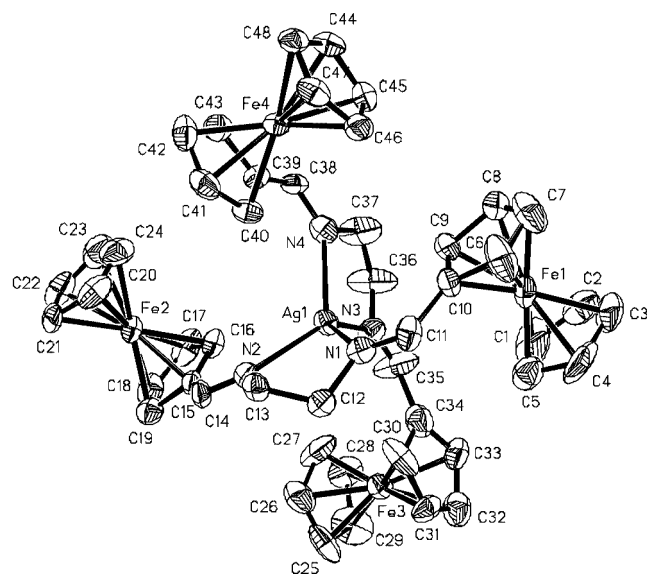


Figure 1. ORTEP drawing with atom-labeling scheme of the cation of $[\text{Ag}(\text{L})_2](\text{NO}_3) \cdot (\text{MeOH}) \cdot (\text{EtOH})$

The Ag^{I} ion is in a distorted tetrahedral environment with the four nitrogen atoms N1, N2, N3 and N4 of two L, which act as bidentate ligands. The Ag–N distances range from 2.277(8) to 2.397(8) Å. The angles N1–Ag1–N2 [77.7(3)°] and N3–Ag1–N4 [77.1(3)°] are acute, and are enforced by the ligand L. The other N–Ag1–N angles are in the range 125.2(3)–130.6(3)°. Hence, the average bond angle at Ag1 is 110.8°, while the dihedral angle between the planes [N1, Ag, N2] and [N3, Ag, N4] is 90.7°. Two five-membered rings, N1–C12–C13–N2–Ag1 and N3–C36–C37–N4–Ag1, adopt λ -conformations (the torsional angles of N1–C12–C13–N2 and N3–C36–C37–N4 are 63.7° and 26.0°, respectively). The geometry at the central Ag^{I} ion is, in fact, the same as that in the related compound $[\text{Cu}(\text{L}^1)_2]\text{BF}_4$ $\{\text{L}^1 = 1,2\text{-bis}[(\text{ferrocen-1-ylmethylene})\text{amino}] \text{benzene}\}$,^[14] which is distorted by the bite of the ferrocenyl ligands.

The average Fe–C_{ring} distance (2.014 Å) is close to that of the free ferrocene (2.04 Å). The average intra C–C bond length of cyclopentadienyl is 1.389 Å, which is shorter than that of the free ferrocene. The average C–C–C angle of 107.8(11)° is similar as those of reported compounds.^[15] In each ferrocenyl moiety, the cyclopentadienyl rings are planar. The dihedral angle between the planes C15–C16–C17–C18–C19 and C20–C21–C22–C23–C24 at Fe2 is 3.5°, and is only 0.7° for the planes C39–C40–C41–

C42–C43 and C44–C45–C46–C47–C48 at Fe4, but the other dihedral angles between the planes C6–C7–C8–C9–C10 and C1–C2–C3–C4–C5 at Fe1 and between the planes C30–C31–C32–C33–C34 and C25–C26–C27–C28–C29 at Fe3 are slightly larger at 6.6° and 7.6°, respectively. The ferrocenyl substituents on each ligand are *transoid*. The dihedral angles between the planes C6–C7–C8–C9–C10 and C10–C11–N1, C15–C16–C17–C18–C19 and C15–C14–N2, C39–C40–C41–C42–C43 and C39–C38–N4, and C30–C31–C32–C33–C34 and C34–C35–N3 are 4.2°, 14.6°, 26.3° and 10.6°, respectively, i.e., the ferrocenyl fragments are not coplanar with the L aldimine groups, unlike those in $[\text{ZnCl}_2(\text{L})]$.^[14] The intramolecular Ag1...Fe1, Ag1...Fe2, Ag1...Fe3, and Ag1...Fe4 distances are 4.772, 4.974, 4.813 and 5.011 Å, respectively, while the Fe1...Fe4, Fe1...Fe3, Fe2...Fe3, and Fe2...Fe4 distances are 6.634, 6.892, 7.153 and 6.977 Å, respectively.

The bond lengths and angles of the nitrate anion are as expected. The average N–O bond length is 1.132 Å, while the average intra-anion angle is 119.9°. The O2 and O3 atoms contribute to the packing by forming hydrogen bonds with crystallization molecules of methanol and ethanol, i.e. two hydrogen bonds arise from the interaction of the OH units in methanol and ethanol with O atoms of the nitrate anion (Figure 2).

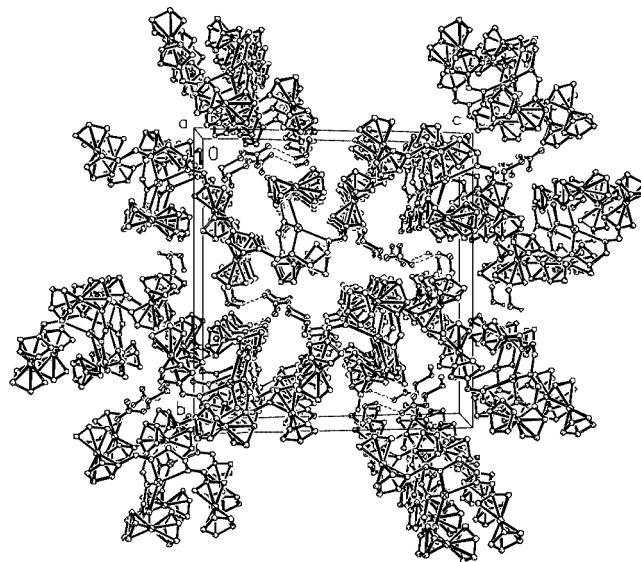


Figure 2. Crystal packing, viewed from the *a* axis, of $[\text{Ag}(\text{L})_2](\text{NO}_3) \cdot (\text{MeOH}) \cdot (\text{EtOH})$

Crystal Structure of $[\text{HgI}_2(\text{L})]$ (2)

An X-ray diffraction analysis of **2** shows that a twofold axis exists in the molecular structure (Figure 3). The center Hg^{II} ion is coordinated by two nitrogen atoms of L and two iodine atoms, forming a distorted tetrahedral geometry, in contrast with the pseudo-tetrahedral zinc(II) center of $[\text{ZnCl}_2(\text{L})]$.^[14] The bond lengths of Hg–N and Hg–I are 2.392(6) and 2.6701(8) Å, respectively, which are close to

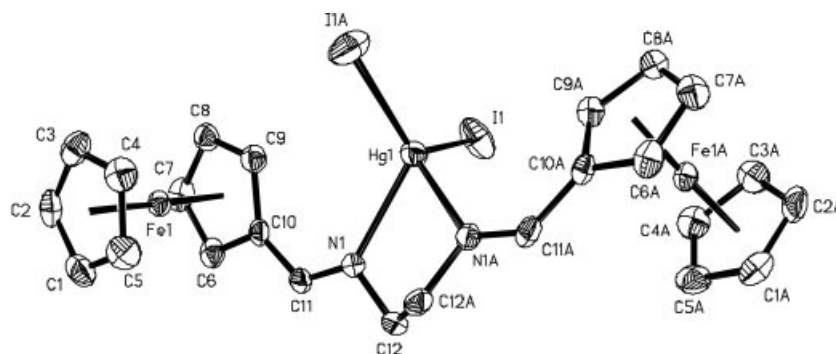


Figure 3. ORTEP drawing with atom-labeling scheme of $[\text{HgI}_2(\text{L})]$

those of the reported coordination polymer $\{\text{HgI}_2[\text{bpmp}]\}_n$ [bpmp = *N,N'*-bis(4-pyridylmethyl)piperazine].^[16] It is interesting that the acute N1-Hg1-N1A angle $[74.5(3)^\circ]$ was enforced by L as is the case for **1**. The widest bond angle around Hg1 is $128.29(4)^\circ$. Hence, the average bond angle at Hg^{II} is 107.5° , while the dihedral angle between the planes $[\text{Hg1}, \text{I1}, \text{I1A}]$ and $[\text{Hg1}, \text{N1}, \text{N1A}]$ is 76.7° . For $[\text{ZnCl}_2(\text{L})]$ the reported N(1)-Zn(1)-N(2) bond angle is 84.3° , and the dihedral angle between $[\text{Zn(1)}, \text{Cl(1)}, \text{Cl(2)}]$ and $[\text{Zn(1)}, \text{N(1)}, \text{N(2)}]$ is 87.3° .

As with compound **1**, the ferrocenyl substituents are in a *transoid* arrangement and not coplanar with the L aldimine groups (the dihedral angle between the planes C6-C7-C8-C9-C10 and C10-C11-N1 is 11.0°). The cyclopentadienyl rings in each ferrocenyl fragment are planar and nearly parallel, with a dihedral angle of 2.2° . $\text{Fe-C}_{\text{ring}}$ distances range from $2.023(6)$ to $2.072(8)$ Å (average 2.04 Å) and intra-cyclopentadienyl C-C bond lengths lie in the range $1.400(12)$ – $1.441(11)$ Å (average 1.42 Å); the C-C-C angles [average $108.0(5)^\circ$] of the ferrocenyl units are all similar to those reported in the literature.^[15] The

intermetallic distances $\text{Hg1}\cdots\text{Fe1}$ and $\text{Fe1}\cdots\text{Fe1A}$ are 5.09 and 10.074 Å, respectively. The molecular packing is shown in Figure 4. The molecules are staggered, on viewing from the *c* axis, and the distance between neighboring Cp groups of different molecules is 3.622 Å, indicating π - π interactions. On the *ab* plane the molecules intercross.

Spectroscopic Properties

The major IR peaks of the two compounds are consistent with the structural results. The characteristic IR bands of the ferrocenyl group at 3100 and 486 cm^{-1} due to $\nu(\text{C-H})$ and $\nu(\text{Fe-Cp})$ vibrations, respectively, are close to those of previously reported compounds.^[11,15a] The imine stretching $\nu(\text{C=N})$ shows a strong absorption at 1640 cm^{-1} in **1** and 1627 cm^{-1} in **2**. The strong absorption at 1384 cm^{-1} could be assigned to the N-O stretching mode of nitrate for **1**.

We found previously^[17,18] that ferrocene exhibits two characteristic absorptions in the UV/Vis spectra at 440 nm (assigned to the $^1\text{E}_{1g} \leftarrow ^1\text{A}_{1g}$ transition) and 325 nm (assigned to the $^1\text{E}_{2g} \leftarrow ^1\text{A}_{1g}$ transition). Complexes **1** and **2** (in DMF) show three characteristic bands. The two absorptive peaks at 325 nm and 447 nm indicate a slight red-shift compared to free ferrocene. The effective bands at 275 nm of **1** and at 271 nm for **2** may be attributed to metal-ligand charge transfer (MLCT) transitions. Both compounds have a relatively low linear absorption, ranging from 500 to 1000 nm, promising low intensity loss and little temperature change due to photon absorption when light propagates in the materials.

The ^1H NMR spectra exhibit signals at $\delta = 8.49, 4.97, 4.53, 4.24\text{--}4.18, 3.72$ ppm (for **1**) and $8.42, 4.83, 4.53, 4.30\text{--}4.27, 3.69$ ppm (for **2**), which are similar to those of ligand L of $\delta = 8.19, 4.64, 4.36, 4.17$, and 3.79 ppm.^[12]

NLO Properties

The NLO determinations revealed that compounds **1** and **2** exhibit very strong nonlinear optical absorption and strong refractive effects.

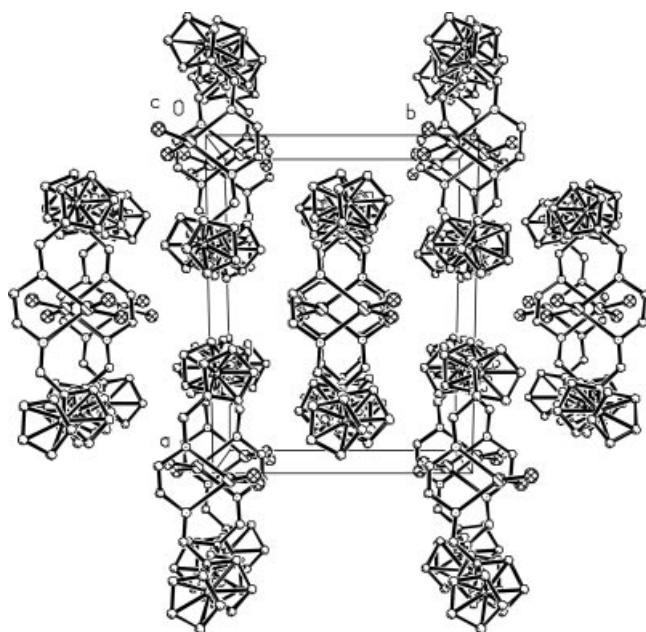


Figure 4. Crystal packing, viewed from the *c* axis, of $[\text{HgI}_2(\text{L})]$

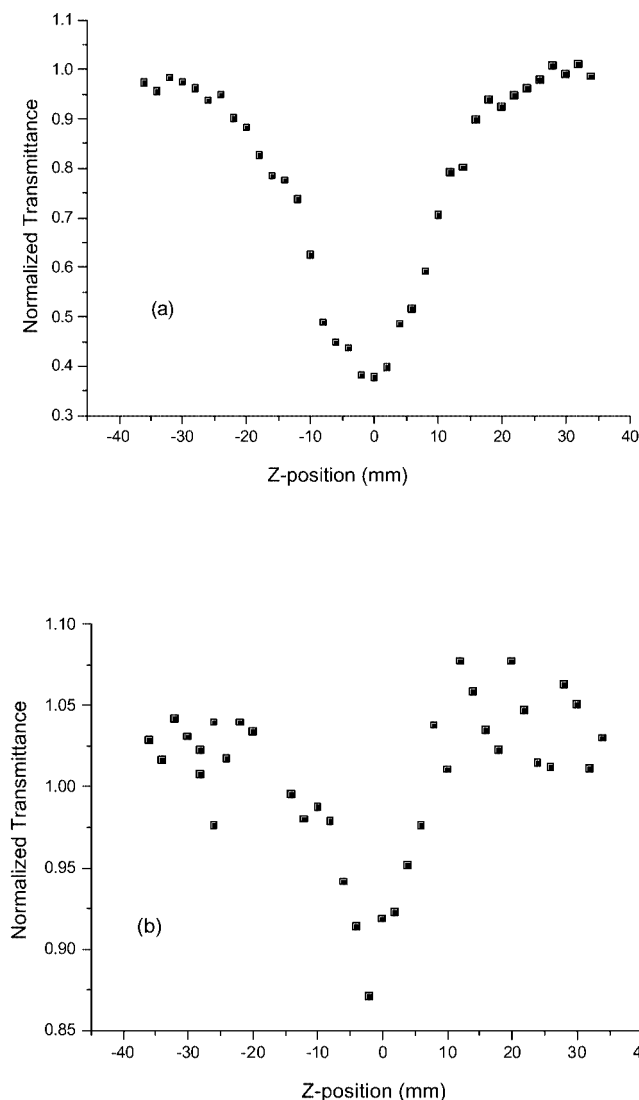


Figure 5. Data were collected under an open aperture configuration at 532 nm; (a; top) NLO absorptive behavior of $[\text{Ag}(\text{L}_2)(\text{NO}_3) \cdot (\text{MeOH}) \cdot (\text{EtOH})]$ in $8.5 \times 10^{-4} \text{ mol} \cdot \text{dm}^{-3}$ DMF solution; (b; bottom) NLO absorptive behavior of $[\text{HgI}_2(\text{L})]$ in $1.9 \times 10^{-3} \text{ mol} \cdot \text{dm}^{-3}$ DMF solution

Figure 5(a and b) depict the NLO absorptive properties of complexes **1** and **2**, respectively. In Figure 5(a) the normalized transmittance drops to about 36% at the focus, showing that **1** has a strong NLO absorptive effect. The third-order NLO absorptive coefficient a_2 is $1.34 \times 10^{-8} \text{ m W}^{-1}$. In Figure 5(b), the normalized transmittance of **2** drops to about 86% at the focus, and the corresponding a_2 value is $3.1 \times 10^{-9} \text{ m W}^{-1}$. The NLO parameters of some known compounds are listed in Table 3, which shows that both **1** and **2** exhibit very strong NLO absorption, and that the a_2 values are larger than those of the reported compounds.^[19–23]

Figure 6(a and b) give the NLO refractive effects of the two complexes; they have a similar positive sign for the refractive nonlinearity, which gives rise to self-focusing behavior. Figure 6(a) shows that the difference between valley-peak positions, $\Delta Z_{\text{V-P}}$, is 19 mm, and the difference between

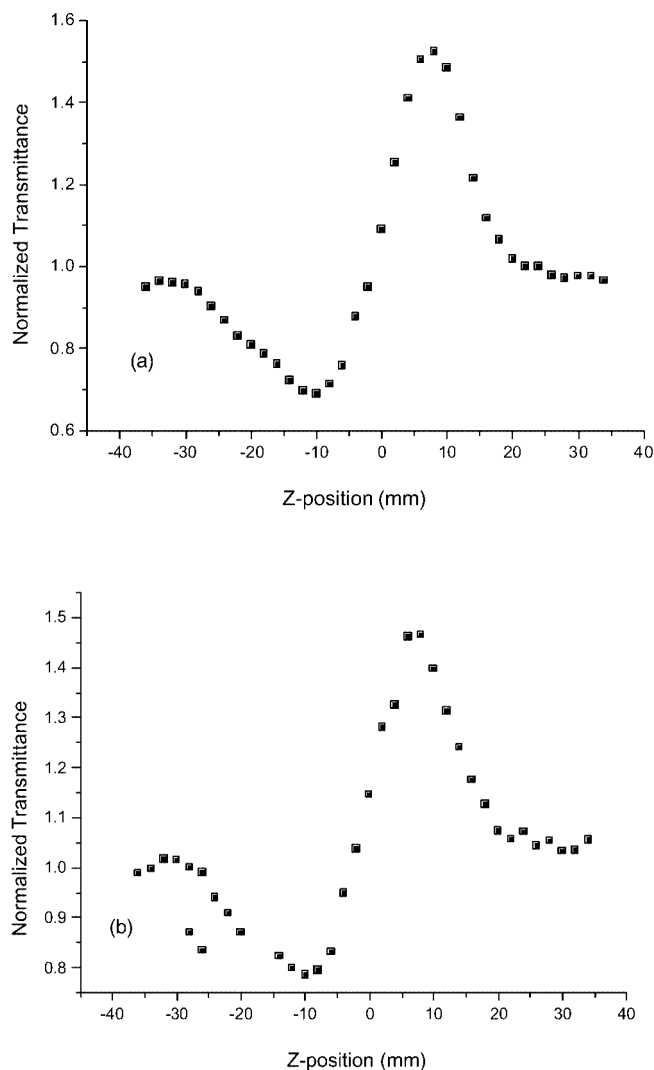


Figure 6. Data were assessed by dividing the normalized Z-scan data obtained under the closed aperture configuration by the normalized Z-scan data obtained under the open aperture configuration; self-focusing effects of (a; top) $[\text{Ag}(\text{L}_2)(\text{NO}_3) \cdot (\text{MeOH}) \cdot (\text{EtOH})]$ in $8.5 \times 10^{-4} \text{ mol} \cdot \text{dm}^{-3}$ DMF solution at 532 nm and (b; bottom) $[\text{HgI}_2(\text{L})]$ in $1.9 \times 10^{-3} \text{ mol} \cdot \text{dm}^{-3}$ DMF solution at 532 nm

normalized transmittance values at valley and peak portions, $\Delta T_{\text{V-P}}$, is 0.86. The refractive index n_2 of **1** is calculated to be $1.15 \times 10^{-18} \text{ m}^2 \text{ W}^{-1}$. According to Figure 6(b), $\Delta Z_{\text{V-P}}$ and $\Delta T_{\text{V-P}}$ are 16 mm and 0.70, respectively, so that $n_2 = 8.02 \times 10^{-19} \text{ m}^2 \text{ W}^{-1}$ is obtained for **2**. Thus, both **1** and **2** have strong self-focusing behavior; similar refractive effects have been found for the clusters $\text{MoCu}_2\text{OS}_3(\text{PPh}_3)_3$, $\text{W}_2\text{Ag}_4\text{S}_8(\text{AsPh}_3)_4$, and $\text{W}_2\text{Ag}_4\text{S}_8(\text{AsPh}_3)_4$.^[20,23]

In accordance with the a_2 and n_2 values, the third-order susceptibility $\chi^{(3)}$ values can be calculated from $|\chi^{(3)}| = \{[(9 \times 10^8 \epsilon_0 n_0^2 c^2 a_2)/2v]^2 + |cn_0^2 n_2/80\pi|^2\}^{1/2}$. The $\chi^{(3)}$ values are $4.11 \times 10^{-12} \text{ esu}$ for **1** and $2.87 \times 10^{-12} \text{ esu}$ for **2**. From the discussions above, we can, reasonably, state that complexes **1** and **2** have similar NLO properties. Most high-performance NLO chromophores, organic polymers^[24–30] and semiconductors^[24–26] are neat materials. Impressive NLO values for ferrocenyl Schiff-base complexes are

achieved with a much diluted solution, and much superior NLO performance can be expected if the solubilities can be improved significantly. We can use the hyperpolarizability γ to represent the NLO properties of neat materials; $\gamma = \chi^{(3)}/NF^4$, where N is the number density of a ferrocenyl complex in the sample (in cm^{-3}), and $F^4 = 3$ is the local field correction factor. Thus γ for compounds **1** and **2** are calculated to be 2.68×10^{-30} and 1.44×10^{-30} esu, respectively.

Molecules possessing extensively conjugated π -electron systems exhibit large optical nonlinearities, especially third-order as described by the second hyperpolarizability, γ .^[31] The γ values of aryl and vinyl of ferrocene increase strongly with the length of the conjugated π -electron system (ranging from $1.61 \pm 0.18 \times 10^{-35}$ to $1.550 \pm 0.270 \times 10^{-33}$ esu).^[31] Compared with the ferrocene derivatives, the γ values of ferrocenyl complexes **1** and **2** are several orders of magnitude larger. A reasonable explanation for this is that the ferrocenyl Schiff-base ligands in the title complexes bearing extended conjugated systems can influence the optical nonlinearity, and the heavy transition metals (Ag, Hg and Fe) may contribute to the optical nonlinearity due to the tailorability of the metal–ferrocenyl ligand interactions. The γ values of our complexes are also similar to those of the ferrocenyl complexes 1,8-bis(ferrocenyl)octatetrayne^[32] and NiL_2 and PdL_2 [$\text{L}^2 = \text{FcC}(\text{CH}_3)=\text{N}_2\text{HCS}_2\text{-CH}_2\text{C}_6\text{H}_5$].^[33] To our knowledge, there have been no reports on third-order NLO properties of diferrocenyl Schiff-base complexes. We believe that our explorations may provide a useful channel to seek new third-order NLO materials.

Experimental Section

General: All chemicals were of reagent-grade quality obtained from commercial sources and used without further purification. 1,2-Bis[(ferrocenyl-ylmethylene)amino]ethane (L) was prepared accord-

ing to the literature method.^[12] IR data were recorded with a Nicolet NEXUS 470-FTIR spectrophotometer with KBr pellets in the 400–4000 cm^{-1} region. UV/Vis spectra were performed with an HP 8453 spectrophotometer. Elemental analyses (C, H and N) were carried out with a Carlo–Erba 1106 Elemental Analyzer. ^1H NMR spectra were recorded at room temperature with a Bruker DPX 400 spectrometer.

Synthesis of $[\text{Ag}(\text{L})_2](\text{NO}_3) \cdot (\text{MeOH}) \cdot (\text{EtOH})$ (1**):** A solution of L (90.3 mg, 0.20 mmol) in ethanol (3 mL) was added dropwise to a solution of AgNO_3 (17.0 mg, 0.10 mmol) in methanol (2 mL). The resulting solution was allowed to stand at room temperature in the dark. Dark-red crystals suitable for X-ray single crystals analysis were obtained over 24 h. Yield: 66.1 mg (61%). Crystals of **1** are unstable in the air. IR: $\tilde{\nu} = 2830$ m, 1640 s, 1384 s, 1247 m, 1104 m, 1013 m, 819 m, 518 m, 510 m, 486 cm^{-1} . $\text{C}_{51}\text{H}_{58}\text{AgFe}_4\text{N}_5\text{O}_5$ (1152.3): calcd. C 53.11, H 5.03, N 6.07; found C 52.45, H 4.80, N 6.21. ^1H NMR (400 MHz, DMSO): $\delta = 8.49$ (s, 4 H, N=CH), 4.97 (s, 8 H, C_5H_4), 4.53 (s, 8 H, C_5H_4), 4.24–4.18 (s, 20 H, C_5H_5), 3.72 (s, 8 H, CH_2).

Synthesis of $[\text{HgI}_2(\text{L})]$ (2**):** L (90.3 mg, 0.20 mmol) in ethanol (3 mL) was slowly added to a solution of HgI_2 (45.60 mg; 0.1 mmol) in DMSO (2 mL) at room temperature. After allowing the resulting mixture to stand in the dark for 2 d, dark-red crystals of **2** suitable for X-ray structure determination were formed. Yield 52.2 mg (57%). **2** is air-stable. IR: $\tilde{\nu} = 1627$ s, 1437 m, 1371 m, 1254 m, 1105 m, 1030 m, 820 m, 510 m, 487 cm^{-1} . $\text{C}_{24}\text{H}_{24}\text{HgFe}_2\text{N}_2\text{I}_2$ (906.6): calcd. C 31.77, H 2.65, N 3.09; found C 32.04, H 2.78, N 2.93. ^1H NMR (400 MHz, DMSO): $\delta = 8.42$ (s, 2 H, N=CH), 4.83 (s, 4 H, C_5H_4), 4.53 (s, 4 H, C_5H_4), 4.30–4.27 (s, 10 H, C_5H_5), 3.69 (s, 4 H, CH_2).

X-ray Crystallographic Study: Crystal data and experimental details for compounds **1** and **2** are contained in Table 1. All measurements were made with a Rigaku RAXIS-IV imaging plate area detector with graphite-monochromated Mo-K_α radiation ($\lambda = 0.71073$ Å). All data were collected at 291(2) K for **1** and 293(2) K for **2** using the ω -2 θ scan technique and correction was applied for Lorentz polarization effects. A correction for secondary extinction was also applied. The two structures were solved by direct methods and ex-

Table 1. Crystal data and structure refinement for $[\text{Ag}(\text{L})_2](\text{NO}_3)(\text{MeOH})(\text{EtOH})$ (**1**) and $[\text{HgI}_2(\text{L})]$ (**2**)

	1	2
Empirical formula	$\text{C}_{51}\text{H}_{58}\text{AgFe}_4\text{N}_5\text{O}_5$	$\text{C}_{24}\text{H}_{24}\text{Fe}_2\text{HgN}_2\text{I}_2$
M	1152.29	906.54
Crystal system	monoclinic	monoclinic
Space group	$P2_1/n$	$C2/c$
a [Å]	12.382 (2)	15.726(3)
b [Å]	21.872(4)	11.809(2)
c [Å]	20.945(4)	14.326(3)
β [°]	102.64(3)	107.82(3)
V [Å ³]	5088.2(18)	2532.7(9)
$D_{\text{calcd.}}$ [mg m^{-3}]	1.504	2.377
T [K]	291(2)	293(2)
Z	4	4
$\mu(\text{Mo-K}_\alpha)$ [mm ⁻¹]	1.541	9.629
Reflections; unique; $R(\text{int})$	8728; 5583; 0.0546	4371; 2447; 0.0498
Data; restraints; parameters	5583; 61; 597	2447; 0; 150
Goodness-of-fit on F^2	1.136	1.079
Final R , ^[a] R_w , ^[b] [$I > 2\sigma(I)$]	0.0891, 0.1999	0.0429, 0.0789
R (all data)	0.1674, 0.2313	0.0559, 0.0828

^[a] $R = \Sigma||F_o| - |F_c||/\Sigma|F_o|$. ^[b] $R_w = [\Sigma(|F_o| - |F_c|)^2/\Sigma w|F_o|^2]^{1/2}$.

Table 2. Selected bond lengths [Å] and bond angles [°] for **1** and **2**Symmetry transformations used to generate equivalent atoms: #1 $-x + 1, y, -z + 1/2$.[Ag(L)₂](NO₃)(MeOH)(EtOH) (**1**)

Ag(1)–N(3)	2.277(8)	N(5)–O(2)	1.087(16)
Ag(1)–N(2)	2.330(7)	N(5)–O(1)	1.105(12)
Ag(1)–N(4)	2.357(7)	N(5)–O(3)	1.205(16)
Ag(1)–N(1)	2.397(8)	N(2)–C(14)	1.265(11)
N(1)–C(12)	1.478(10)	C(14)–C(15)	1.448(13)
N(2)–C(13)	1.519 (11)	N(1)–C(11)	1.294(12)
C(12)–C(13)	1.491 (13)	C(11)–C(10)	1.470(14)
N(3)–C(36)	1.408(12)	N(3)–C(35)	1.224(13)
C(36)–C(37)	1.400(12)	N(4)–C(38)	1.295(11)
N(4)–C(37)	1.481 (12)	C(38)–C(39)	1.422(13)
C(35)–C(34)	1.706(18)		
N(3)–Ag(1)–N(2)	130.6(3)	N(3)–Ag(1)–N(1)	128.0(3)
N(3)–Ag(1)–N(4)	77.1(3)	N(2)–Ag(1)–N(1)	77.7(3)
N(2)–Ag(1)–N(4)	126.1(3)	N(4)–Ag(1)–N(1)	125.22(3)
Ag(1)–N(1)–C(12)	104.2(6)	Ag(1)–N(2)–C(13)	106.5(5)
Ag(1)–N(3)–C(36)	111.9(6)	Ag(1)–N(4)–C(37)	106.9(6)
[HgI ₂ (L)] (2)			
Hg(1)–N(1)	2.392(6)	Hg(1)–I(1)	2.6701(8)
N1–C11	1.285(8)	C12–C12#1	1.530(17)
N1–C12	1.459(9)	C10–C11	1.436(10)
N(1)–Hg(1)–N(1)#1	74.5(3)	N(1)–Hg(1)–I(1)#1	118.18(13)
N(1)–Hg(1)–I(1)	102.82(14)	N(1)#1–Hg(1)–I(1)#1	102.82(14)
N(1)#1–Hg(1)–I(1)	118.18(13)	I(1)–Hg(1)–I(1)#1	128.29(4)
C10–C11–N1	126.1(7)	N1–C12–C12#1	109.5(5)
C11–N1–Hg1	132.2(5)	C12–N1–Hg1	108.1(4)
C11–N1–C12	119.3(6)	C11–C10–C9	129.5(6)
C11–C10–C6	1236.6(7)		

Table 3. Optical parameters of selected NLO chromophores

Compounds	C [mol·dm ^{−3}]	α_2 [m W ^{−1}]	n_2 [m ² W ^{−1}]	$\chi^{(3)}$ [esu]	γ [esu]	Ref.
Cluster compounds:						
WOS ₃ Cu ₃ (SCN)(Py) ₅	1.9×10^{-5}	6.0×10^{-11}	-1.2×10^{-17}	8.0×10^{-11}	2.2×10^{-27}	[19]
MoOS ₃ Cu ₃ (SCN)(Py) ₅	2.0×10^{-5}	4.8×10^{-10}	-6.8×10^{-17}	2.0×10^{-10}	5.8×10^{-27}	[19]
MoCu ₂ OS ₃ (PPh ₃) ₃	7.4×10^{-5}	2.6×10^{-10}	5.0×10^{-17}	1.2×10^{-10}	9.8×10^{-28}	[20]
WCu ₂ OS ₃ (PPh ₃) ₄	1.2×10^{-4}		8.0×10^{-18}	2.0×10^{-11}	9×10^{-29}	[20]
[Et ₄ N] ₄ [Mo ₂ O ₂ S ₆ Cu ₆ I ₆]	2.0×10^{-3}	4.0×10^{-10}	-6.0×10^{-17}			[21]
[MoI(bPy) ₂][MoOS ₃ Cu ₃ I ₂ (bPy)]	3.4×10^{-5}	3.0×10^{-10}	-3.0×10^{-17}			[22]
[WI(bPy) ₂][MoOS ₃ Cu ₃ I ₂ (bPy)]	4.8×10^{-5}	1.0×10^{-9}				[22]
[MoOS ₃ Cu ₃ I(bMe-bPy) ₂]	2.4×10^{-5}	3.5×10^{-10}				[22]
W ₂ Ag ₄ S ₈ (AsPh ₃) ₄	1.3×10^{-4}	2.8×10^{-9}	5.9×10^{-17}	1.7×10^{-10}		[23]
Organic polymers:						
PA	neat			5.0×10^{-10}		[24–26]
PDA-PTS	neat			8.5×10^{-10}		[24–26]
PDA-4BCMU	neat			1.8×10^{-10}		[24–26]
Polyarylenes	neat			10^{-11} to 10^{-9}		[27]
σ-Conjugated polymers	neat			10^{-12} to 10^{-11}		[28,29]
Organic ladder polymers	neat			10^{-11} to 10^{-10}		[30]
Semiconductors:						
GaAs	neat			4.8×10^{-11}		[24–26]
Ge	neat			4.0×10^{-10}		[24–26]
Ferrocenyl complexes:						
1,8-Bis(ferrocenyl)octatetrayne					1.10×10^{-32}	[32]
NiL ₂ (L ² =FcC(CH ₃)=N ₂ HCS ₂ CH ₂ C ₆ H ₅)				1.60×10^{-12}	2.71×10^{-33}	[33]
PdL ₂				2.14×10^{-12}	3.06×10^{-33}	[33]
Ferrocene					$1.61 \pm 0.18 \times 10^{-35}$	[31]
Ferrocenecarboxaldehyde					$1.69 \pm 0.08 \times 10^{-35}$	[31]
FcCH=CHC ₆ H ₅					$8.55 \pm 1.98 \times 10^{-35}$	[31]
1,1'–Fc(CH=CHC ₆ H ₅) ₂					$2.70 \pm 0.26 \times 10^{-34}$	[31]
OHC(–FcCH=CHC ₆ H ₅ CH=CH–) _n					$1.55 \pm 0.27 \times 10^{-33}$	[31]
[Ag(L) ₂](NO ₃)(MeOH)(EtOH) (1)	8.5×10^{-4}	1.34×10^{-8}	1.15×10^{-18}	4.11×10^{-12}	2.68×10^{-30}	this work
[HgI ₂ (L)] (2)	1.1×10^{-3}	3.1×10^{-9}	8.02×10^{-19}	2.87×10^{-12}	1.44×10^{-30}	this work

panded using the Fourier technique. The non-hydrogen atoms were found by successive full-matrix least-squares refinement on F^2 and refined with anisotropic thermal parameters. Hydrogen atoms were included but not refined. All calculations were performed using the SHELX-97 crystallographic software package.^[34] Selected bond lengths and bond angles are listed in Table 2. CCDC-178522 (**1**) and -178521 (**2**) contain the supplementary crystallographic data for this paper. These data can be obtained free of charge at www.ccdc.cam.ac.uk/conts/retrieving.html [or from the Cambridge Crystallographic Data Centre, 12 Union Road, Cambridge CB2 1EZ, UK; Fax: (internat.) + 44-1223/336-033; E-mail: deposit@ccdc.cam.ac.uk].

NLO Measurements: The third-order NLO properties were measured by the Z-scan technique^[35] with a 532-nm laser pulse of 8 ns duration in a solution of 8.5×10^{-4} mol·dm⁻³ (for **1**) and 1.1×10^{-3} mol·dm⁻³ (for **2**) (the different concentrations are due to the different solubilities of the two complexes in DMF). The NLO absorption components were evaluated by a Z-scan experiment under an open-aperture configuration. Light transmittance (T) is a function of incident light irradiance $I(Z)$, nonlinear absorption [$a_2 = a_2(I_1)$], and linear absorption (a_0) as illustrated in Equations (1) and (2).^[35b] The NLO absorption data of the two complexes can be well represented by Equations (1) and (2), where Z is the distance of the sample from the focal point; a_0 and a_2 are the linear and nonlinear absorption coefficients, respectively; L is the sample thickness (1 mm in this study); I_0 is the peak irradiation intensity at focus; $Z_0 = \pi\omega_0^2/\lambda$ where ω_0 is the spot radius of the laser beam at focus, and λ is the wavelength of the laser; r is the radial coordinate; t is the time; and t_0 is the pulse width.

$$T(Z) = \frac{1}{\sqrt{\pi}q(Z)} \int_{-\infty}^{\infty} \ln[1 + q(Z)]e^{-t^2} dt \quad (1)$$

$$q(Z) = \int_0^L \int_0^\infty \alpha_2 \frac{I_0}{1 + (Z/Z_0)^2} e^{[-2(\gamma/\omega_0)^2 - (t/t_0)^2]} \frac{1 - e^{-\alpha_0 L}}{\alpha_0} r dr dt \quad (2)$$

The NLO refractive effects were assessed by dividing the normalized Z-scan data obtained under the closed-aperture configuration by the normalized Z-scan data obtained under the open aperture configuration. An effective third-order NLO refractive index n_2 can then be derived by Equation (3), where ΔT_{V-P} and is the difference between normalized transmittance values at valley and peak positions; I is the peak irradiation intensity at focus. Table 3 gives the γ values of some reported NLO materials.

$$n_2 = \frac{\lambda \alpha_0}{0.812\pi(1 - e^{-\alpha_0 L})} \Delta T_{V-P} \quad (3)$$

Acknowledgments

The authors thank the National Natural Science Foundation of China, Outstanding Young Teacher Foundation of Ministry of Education of China and the Outstanding Younger Foundation of Henan Province for financial support.

- [1] A. Togni, T. Hayashi, *Ferrocenes. Homogenous Catalysis, Organic Synthesis, Materials Science*, VCH, Weinheim, Germany, 1995.
 [2] R. W. Wagner, P. A. Johnson, J. S. Lindsey, *J. Chem. Soc., Chem. Commun.* **1991**, 1463–1466.
 [3] J. S. Miller, A. J. Epstein, *Angew. Chem. Int. Ed. Engl.* **1994**, 33, 385–415.

- [4] [4a] P. Nguyen, P. Gómez-Elipe, I. Manners, *Chem. Rev.* **1999**, 99, 1515–1548. [4b] S. Barlow, D. O'Hare, *Chem. Rev.* **1997**, 97, 637–669. [4c] D. R. Kanis, M. A. Ratner, T. J. Marks, *Chem. Rev.* **1994**, 94, 195–242. [4d] N. J. Long, *Angew. Chem. Int. Ed. Engl.* **1995**, 34, 21–38. [4e] T. Verbiest, S. Houbrechets, M. Kaurann, K. Clays, A. Persoons, *J. Mater. Chem.* **1997**, 7, 2175–2189. [4f] I. Cuadrado, M. Morán, C. M. Casado, B. Alonso, J. Losada, *Coord. Chem. Rev.* **1999**, 193–195, 395–445. [4g] G. G. A. Balavione, J.-C. Daran, G. Iftime, P. G. Lacroix, E. Manoury, J. A. Delaire, I. Maltey-Fanton, K. Nakatani, S. D. Bella, *Organometallics* **1999**, 18, 21–29. [4h] M. Blanchard-Desce, C. Runser, A. Fort, M. Barzoukas, J. M. Lehn, V. Alain, *Chem. Phys.* **1995**, 199, 253–261.
 [5] M. L. H. Green, S. R. Marder, M. E. Thompson, J. A. Bandy, D. Bloor, P. V. Kolinsky, R. J. Jones, *Nature* **1987**, 330, 360–362.
 [6] A. Houlton, N. Jassim, R. M. G. Roberts, J. Silver, P. McArdle, T. Higgins, *J. Chem. Soc., Dalton Trans.* **1992**, 2235–2241.
 [7] I. Ratera, D. Ruiz-Molina, C. Sánchez, R. Alcalá, C. Rovira, J. Veciana, *Synth. Met.* **2001**, 121, 1834–1835.
 [8] J. Silver, J. R. Miler, A. Houlton, M. T. Ahmet, *J. Chem. Soc., Dalton Trans.* **1994**, 3355–3360.
 [9] A. Houlton, J. R. Miler, J. Silver, N. Jassim, M. T. Ahmet, T. L. Axon, D. Bloor, G. H. Cross, *Inorg. Chim. Acta* **1993**, 205, 67–70.
 [10] S. K. Pal, A. Krishnan, P. K. Das, A. G. Samuelson, *J. Organomet. Chem.* **2000**, 604, 248–259.
 [11] E. W. Nause, M. G. Meirim, N. F. Blom, *Organometallics* **1988**, 7, 2562–2565.
 [12] A. Benito, J. Cano, R. Martínez-Máñez, J. Soto, J. Payá, F. Lloret, M. Julve, J. Faus, M. D. Marcos, *Inorg. Chem.* **1993**, 32, 1197–1203.
 [13] O. Knoesen, H. Görls, S. Lotz, *J. Organomet. Chem.* **2000**, 598, 108–115.
 [14] P. Li, I. J. Scowen, J. E. Davies, M. A. Halcrow, *J. Chem. Soc., Dalton Trans.* **1998**, 3791–3799.
 [15] [15a] E. R. Lippincott, R. D. Nelson, *Spectrochim. Acta* **1958**, 10, 307–309. [15b] F. Takusagawa, T. F. Koetzle, *Acta Crystallogr., Sect. B* **1979**, 35, 2888–2896.
 [16] Y. Y. Niu, H. W. Hou, Y. L. Wei, Y. T. Fan, Y. Zhu, C. X. Du, X. Q. Xin, *Inorg. Chem. Commun.* **2001**, 4, 358–361.
 [17] Y. S. Sohn, D. N. Hendrickson, H. B. Gray, *J. Am. Chem. Soc.* **1971**, 93, 3603–3612.
 [18] A. T. Armstrong, A. T. Smith, E. Elder, S. P. McGlynn, *J. Chem. Phys.* **1967**, 46, 4321–4328.
 [19] H. W. Hou, H. G. Ang, S. G. Ang, Y. T. Fan, M. K. M. Low, W. Ji, Y. W. Lee, *Phys. Chem. Chem. Phys.* **1999**, 1, 3145–3149.
 [20] S. Shi, H. W. Hou, X. Q. Xin, *J. Phys. Chem.* **1995**, 99, 4050–4053.
 [21] H. W. Hou, D. L. Long, X. Q. Xin, X. X. Huang, B. S. Kang, P. Ge, W. Ji, S. Shi, *Inorg. Chem.* **1996**, 35, 5363–5367.
 [22] H. W. Hou, H. G. Ang, S. G. Ang, Y. T. Fan, M. K. M. Low, W. Ji, Y. W. Lee, *Inorg. Chim. Acta* **2000**, 299, 147–154.
 [23] G. Sakane, T. Shibahare, H. W. Hou, X. Q. Xin, S. Shi, *Inorg. Chem.* **1995**, 34, 4785–4789.
 [24] J. L. Bredas, C. Adant, P. Tackx, A. Persoons, B. M. Pierce, *Chem. Rev.* **1994**, 94, 243–278.
 [25] H. Nakanishi, *Nonlinear Optics* **1991**, 1, 223–226.
 [26] T. Kobayashi, *IEICE Trans. Fundam.* **1992**, E75-A, 38–45.
 [27] D. A. Halliday, P. L. Burn, D. D. C. Bradley, R. H. Friend, O. M. Gelsen, A. B. Holmes, A. Kraft, J. H. F. Martens, K. Pichler, *Adv. Mater.* **1993**, 5, 40–44.
 [28] F. Kajzar, J. Messier, C. Rosilio, *J. Appl. Phys.* **1986**, 60, 3040–3044.
 [29] F. Schellenberg, R. L. Byer, R. D. Miller, *Chem. Phys. Lett.* **1990**, 166, 331–339.
 [30] L. Yu, D. W. Polis, M. R. McLean, L. R. Dalton, *In Electroresponsive Molecular and Polymeric Systems* (Ed.: T. A. Skotheim), Marcel Dekker, New York, **1991**, vol. 2.

- [³¹] S. Ghosal, M. Samoc, P. N. Prasad, J. J. Tufariello, *J. Phys. Chem.* **1990**, *94*, 2847–2851.
- [³²] Z. Yuan, G. Stringer, I. R. Jobe, D. Kreller, K. Scott, L. Koch, N. J. Taylor, T. B. Marder, *J. Organomet. Chem.* **1993**, *452*, 115–120.
- [³³] Y. P. Tian, Z. L. Lu, X. Z. You, *Acta Chim. Sin. (Chin. Ed.)* **1999**, *57*, 1068–1074.
- [³⁴] [^{34a}] G. M. Sheldrick, *SHELXS-97*, University of Göttingen, Germany, **1997**; G. M. Sheldrick, *Acta Crystallogr., Sect. A* **1990**, *46*, 467–473. [^{34b}] G. M. Sheldrick, *SHELXL-97*, University of Göttingen, Germany, **1997**.
- [³⁵] [^{35a}] H. W. Hou, X. Q. Xin, J. Liu, M. Q. Chen, S. Shi, *J. Chem. Soc., Dalton Trans.* **1994**, 3211–3214. [^{35b}] M. Sheik-Bahae, A. A. Said, T. H. Wei, D. J. Hagan, E. W. Van Stryland, *IEEE J. Quant. Electron.* **1990**, *26*, 760–769.

Received November 12, 2003